Tetrahedron 67 (2011) 3705–3713

Contents lists available at ScienceDirect

Tetrahedron

journal homepage: www.elsevier.com/locate/tet

Covalent nano-clip and nano-box compounds based on free base porphyrins

Emilio Scamporrino [a], Placido Mineo [a,b,*], Daniele Vitalini [c]

[a] Dipartimento di Scienze Chimiche, Università di Catania, Viale A. Doria 6, 95125 Catania, Italy
[b] Istituto per i Processi Chimico Fisici—CNR, Viale Ferdinando Stagno D'Alcontres 37, 98158 Messina, Italy
[c] Istituto per la Chimica e Tecnologia dei Polimeri, Sezione di Catania—CNR, Via Paolo Gaifami 18, 95126 Catania, Italy

ARTICLE INFO

Article history:
Received 7 January 2011
Received in revised form 26 February 2011
Accepted 21 March 2011
Available online 26 March 2011

Keywords:
Cyclic porphyrin-oligomers
Nano-structure
MALDI-TOF mass spectrometry
UV–vis spectroscopy
NMR spectroscopy

ABSTRACT

Novel nano-clip and nano-box compounds were obtained by reaction between dibromomethane and 5,15-di[*p*-(9-methoxytriethylenenoxy)phenyl]-10,20-di[*p*-hydroxyphenyl]porphyrin. The molecular architecture varies from a co-facial (nano-clip) to a four wall-box (nano-box) structure. The products were characterized by ^{1}H NMR and UV–vis spectroscopy and MALDI-TOF mass spectrometric analysis.
The UV–vis spectra of the nano-clip showed a modification of the characteristic porphyrin soret and Q bands, with respect to the monomer and cyclic tetramer, as a probable consequence of a hybrid orbital deformation (HOD) phenomenon involving the two porphyrin π rings forced to a closer co-facial spatial arrangement. The spatial distance between the two co-facial porphyrin units, and therefore the molecular cavity size, can be modified inducing an electrostatic repulsion by means of a reversible protonation of the pyrrolic cores. The ^{1}H NMR spectra of the nano-box showed a strong high-field shift of some aromatic and ether protons present in the upper and lower rim of the molecular box.

1. Introduction

There is an increasing interest in developing smart nano-structures for applications in many different fields, from environmental monitoring to biological, medical and industrial chemistry. For some specific properties (e.g., strong molar absorption, bound metal atoms in pyrrolic cores, extensive aromatic structures, peculiar affinity for neoplastic cells, etc.), porphyrin derivatives are among the most studied compounds, and some applications like chemical and/or biological receptors, artificial sensors for drug determinations, mimesis of biological systems, etc., are already well-defined.[1–10] Furthermore, because of their tendency to accumulate in cancer cells, some of these synthetic structures have already been tested for drug-delivery in cancerous diseases.

In the presence of the appropriate molecules and/or external stimuli, these systems can change their physicochemical properties in a characteristic and measurable manner (as a consequence of structural modification due to supramolecular complex formation or to chemical alteration) performing, in some cases, a specific task. For instance, some linearly conjugated poly-porphyrins behave like photon nano-wires,[11] whereas cyclic porphyrins, coupled with electron acceptor units (i.e., fullerenes), are used as light-harvesting systems.[12] In addition, some porphyrin structures are used as enzyme mimics,[13] etc.

More recently, several 3D cyclic oligo-porphyrins with different architectures [e.g., spheres, prisms, regular polyhedra (with a varying number of faces), etc.] have been studied.[14–17] The properties of these molecules may depend on the size and hydrophobic nature of the cavities inside their 3D structure[18] (for example, suitable to accommodate hydrophobic chemicals) as well as the presence of functional groups.

We recently reported some work regarding the synthesis of some uncharged water-soluble porphyrins[19] and bis-porphyrins,[20] and the modification of their spectroscopic properties (i.e., NMR, UV–vis and circular dichroism) when treated with aliphatic and aromatic α-L-amino acids.

In particular, it was found that their qualitative bio-molecular recognition properties depend strongly on the porphyrin structure. Mono-porphyrins were tools for the recognition of enantiomeric species and discrimination between aliphatic and aromatic aminoacids,[21,22] while bis-porphyrins, arranged as molecular tweezers, were useful for the recognition of bio-molecules having different sizes.[23]

In the present paper, as the first step in the preparation of water-soluble nano-clip and nano-box compounds, the synthesis and characterization of some novel cyclic ethers, constituted by two (nano-clip) or four (nano-box) porphyrin units and spaced with

* Corresponding author. E-mail address: gmineo@unict.it (P. Mineo).

0040-4020/$ – see front matter © 2011 Elsevier Ltd. All rights reserved.
doi:10.1016/j.tet.2011.03.072

methylene bridges, are reported. These compounds, obtained by the reaction between dibromomethane and 5,15-di[*p*-(9-methoxytriethylenenoxy)phenyl]-10,20-di[*p*-hydroxyphenyl]porphyrin, have a co-facial (nano-clip) or a four wall-box (nano-box) architecture. Planar isomeric cyclic porphyrin ethers, starting from the 5,10-di[*p*-(9-methoxytriethylenenoxy)phenyl]-15,20-di[*p*-hydroxyphenyl] porphyrin, were also prepared to verify the dependence of the spectroscopic data on the molecular arrangement.

The aim of these syntheses was to obtain molecular systems for the recognition and/or the carriage of bio-molecules. Spectroscopic data of the nano-clip showed modified soret and Q-bands, with respect to the monomer and cyclic tetramer. An UV–vis titration allowed verification of the easy and reversible protonation of the pyrrolic cores which, by electrostatic repulsion, modifies the spatial distance between the two co-facial porphyrins and, therefore, the cavity size. This reversible modification could be used to change the dimer molecule status from open to closed, and facilitate the accommodation or release of suitable chemical species, acting then as a drug carrier.

The tetrameric porphyrin molecule (nano-box) could also be used as a drug carrier, forming an inclusion complex with macromolecular drugs, or as a nano-reactor, for the peculiar nano-space conditions inside the box. In this case, ^{1}H NMR spectroscopic analysis showed a high-field shift of the aromatic and ether protons present in the upper and lower box rims as a specific characteristic of this molecular structure.

These compounds differ from previous analogous porphyrinic systems[14–17] in that their totally covalent structure makes them more versatile potential macromolecular tools.

2. Results and discussion

The synthesis of cyclic oligomers containing porphyrin units involved the use of 5,15-di[*p*-(9-methoxytriethyleneoxy)phenyl]-10,20-di[*p*-hydroxyphenyl]porphyrin [indicated as HO(H_2–PTTEG_2)OH] or 5,10-di[*p*-(9-methoxytriethyleneoxy)phenyl]-15,20-di[*p*-hydroxyphenyl]porphyrin [indicated as HO(H_2–PCTEG_2)OH] in turn obtained by the reaction between tetrakis-*p*-(hydroxyphenyl)porphyrin and 9-methyltriethyleneoxy chloride (see Experimental section).

Pure HO(H_2–PTTEG_2)OH and HO(H_2–PCTEG_2)OH were collected by chromatographic separation and their exact identification was achieved examining their MALDI-TOF mass spectrometric and NMR spectra. In Fig. 1, the ^{1}H NMR spectra of the third and fourth coloured product eluted from the chromatographic column are compared which, both with a molecular ion at *m*/*z* 971 (as MH^+), were identified as the two isomeric 10,20- and 15,20-di(*p*-hydroxyphenyl)porphyrin derivatives.

On the basis of some marked differences, spectrum (a) was assigned as the centre-symmetrical [HO(H_2–PTTEG_2)OH] isomer (see inset in Fig. 1a) for which the following characteristic signals have been recorded: a signal at 8.87 ppm (8H, pyrrole protons 2, 3, 7, 8, 12, 13, 17, 18); a doublet at 8.12 ppm (4H, phenyl protons a); a doublet at 8.08 ppm (4H, phenyl protons a′); a doublet at 7.31 (4H, CH phenyl protons b); a doublet at 7.23 (4H, CH phenyl protons b′); a broad triplet at 4.42 ppm (4H, methylene protons c); broad triplet at 4.045 ppm (4H, methylene protons d); four broad triplets, range 3.86–3.72 ppm (16H, methylenes e, f, g, h); a singlet at 3.42 ppm (6H, terminal methyl groups ω); a singlet at −2.78 ppm (2H, N–H pyrrole protons 21, 22). In particular, the collapse of the doublet signals can be observed due to 2–3, 7–8, 12–13 and 17–18 in the same unresolved peak (at 8.87 ppm).

These assignments are also supported by T-ROESY [omitted for brevity, which shows the diagnostic cross-peak correlations between protons c–b; a–(3, 7, 13, 17) and a′–(8, 12, 2, 18)] and COSY [omitted for brevity, which shows cross-peak correlations between the signals of the a–b, a′–b′, c–d, e–f and g–h protons] experiments.

The ^{1}H NMR spectrum of HO(H_2–PCTEG_2)OH, reported in Fig 1b together with the molecular structure of the monomer as an inset, is similar to that of HO(H_2–PTTEG_2)OH but, because of its lower symmetry, the CH pyrrole signals 2, 3, 7, 8, 12, 13, 17, 18 are present as a characteristic cluster at about 8.8 ppm. Considering the structure reported as an inset in Fig 1b, the T-ROESY experiment (omitted for brevity) showed the diagnostic cross-peak correlations between protons c–b; a′–(17, 18); a–(7, 8); a′–(2, 13) and a–(3, 12) whereas the COSY experiment (omitted for brevity also) highlighted the cross-peak correlations between a–b, a′–b′, c–d; e–f and g–h protons. All the data indicate HO(H_2–PTTEG_2)OH and the HO(H_2-PCTEG_2)OH as the third and the fourth coloured products, respectively, eluted from the chromatographic column.

To promote the formation of oligomeric species, the syntheses of cyclic porphyrins were performed by reacting HO(H_2–PTTEG_2)OH or HO(H_2–PCTEG_2)OH with dibromomethane in diluted conditions (see Experimental part).

MALDI-TOF mass spectra of the final products of both reactions between dibromemethane and HO(H_2–PTTEG_2)OH or HO(H_2–PCTEG_2)OH are showed in Fig. 2.

Both spectra only show signals corresponding to the molecular ions of cyclic cy-[O–(H_2–PTTEG_2)–O–CH_2–]$_n$ and or cy-[O–(H_2–PCTEG_2)–O–CH_2–]$_n$ oligomers (Scheme 1, with n=2–8) detected as MH^+ (more intense signals, *m*/*z* values and compositions are reported in the spectra), MNa^+ and MK^+ species. In particular, the peak of the cyclic tetramer is the most abundant species formed in the reaction with 10,20-di[*p*-hydroxyphenyl]porphyrin (Fig. 2a) whereas the cyclic dimer is the most abundant species formed when 15,20-di[*p*-hydroxyphenyl]porphyrin is used (Fig. 2b).

Pure oligomers were obtained by chromatographic column fractionation and, as an example, the MALDI-TOF spectra of cyclic methylene-ether dimer cy-[O–(H_2–PCTEG_2)–O–CH_2–]$_2$ (obtained with a yield of 30%) and cyclic methylene-ether tetramer cy-[O–(H_2–PTTEG_2)–O–CH_2–]$_4$ (yield of 18%) are shown in Fig. 3a and b, respectively.

The structure of cy-[O–(H_2–PCTEG_2)–O–CH_2–]$_2$ was confirmed by ^{1}H NMR, COSY and T-ROESY experiments. In particular, as reported in Fig. 4, the ^{1}H NMR spectrum shows the following signals (for the assignments see Scheme 2): a doublet at 9.13 ppm (4H, C–H pyrrole protons 8, 17); a doublet at 8.99 ppm (4H, C–H pyrrole protons 7, 18); a singlet at 8.93 ppm (4H, C–H pyrrole protons 2, 3); a singlet at 8.72 ppm (4H, C–H pyrrole protons 12, 13); a doublet at 8.22 ppm (8H, phenyl protons a′); a doublet at 8.19 ppm (8H, phenyl protons a); a doublet at 7.69 (8H, phenyl protons b′); a doublet at 7.38 (8H, phenyl protons b); a singlet at 6.41 ppm (4H, methylene bridge protons c′); a broad triplet at 4.48 ppm (8H, methylene protons c); a triplet at 4.08 ppm (8H, methylene protons *d*); a triplet, range 3.89–3.63 ppm (32H, methylene protons *e*, *f*, *g*, *h*); a singlet at 3.44 ppm (12H methyl protons ω); a singlet at −2.73 ppm (4H, N–H pyrrole protons 21, 22).

The ^{1}H NMR signal attributions were supported by T-ROESY [Supplementary data, Fig. 1 in which the cross-peaks correlation between protons a–(2,3); a–(7,18); b–c; a′–(8,17); a′–(12,13); b′–c′ are shown] and COSY [Supplementary data, Fig. 2 that shows the cross-peaks correlation between protons a–b; c–d; (7,18)–(8,17) and a′–b′] experiments.

The ^{1}H NMR spectrum of cy-[O–(H_2–PTTEG_2)–O–CH_2–]$_4$, Fig 5, shows some signals having anomalous chemical shift values. In particular (for the assignments see Scheme 3): a doublet at 8.80 ppm (16H, C–H pyrrole protons 8, 12–2, 18); a doublet at 8.29 ppm (16H, phenyl protons a′); a doublet at 8.24 ppm (16H, C–H pyrrole protons 3, 7–13, 17); a doublet at 7.68 ppm (16H, phenyl protons b′); a broad peak at 6.83 ppm (16H, phenyl protons

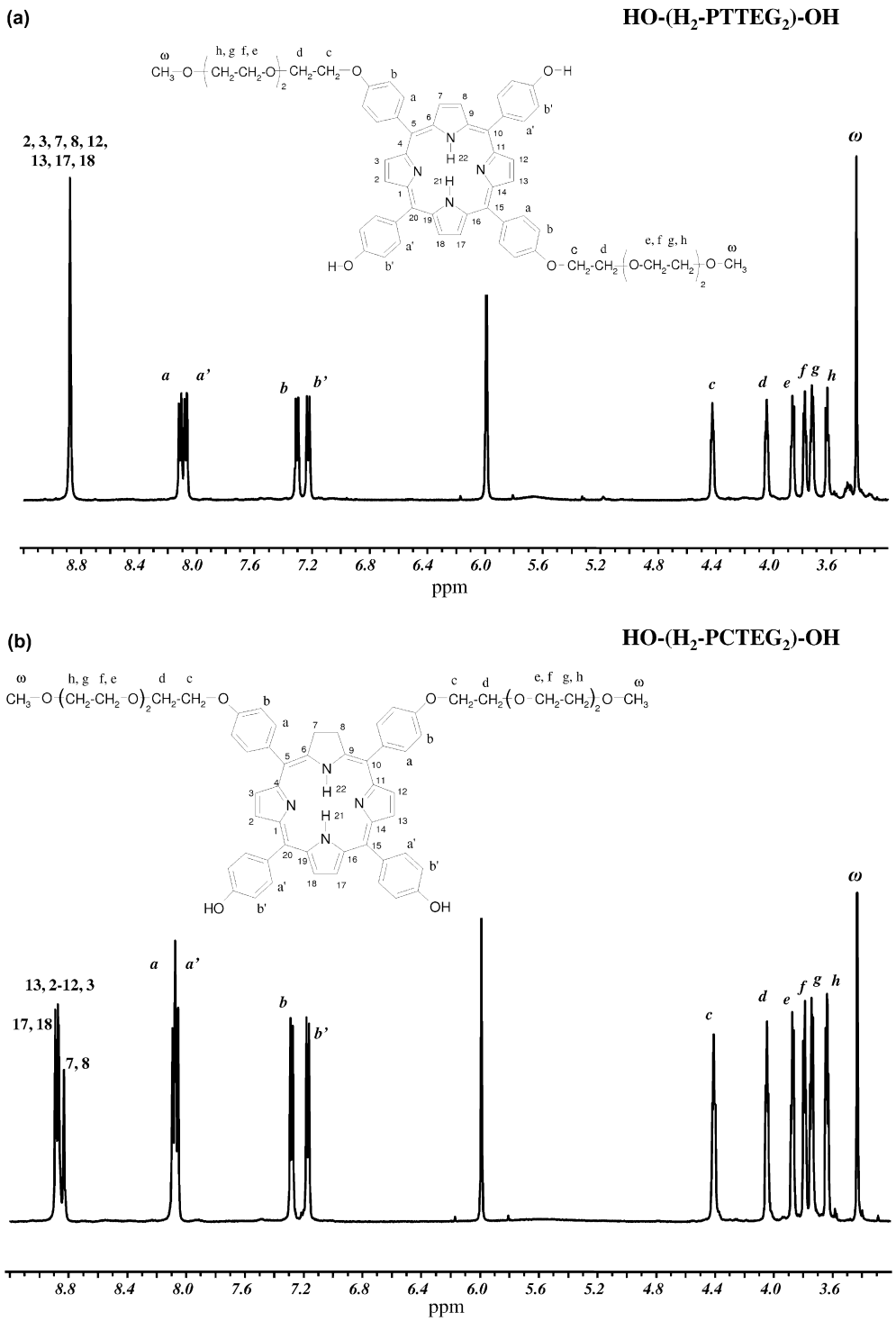

Fig. 1. ^{1}H NMR spectra ($CDCl_2CDCl_2$, 500 MHz) of: (a) HO(H_2–PTTEG$_2$)OH; (b) HO(H_2–PCTEG$_2$)OH.

a); a singlet at 6.39 ppm (8H, methylene bridge protons c′); a broad peak at 5.80 ppm (16H, phenyl protons b); a multiplet in the range 3.69–3.57 ppm (80H, methylene protons d, e, f, g, h); a singlet at 3.38 ppm (24H, methyl protons ω); a broad peak at 3.18 ppm (16H, methylene protons c); a singlet at −2.69 ppm (8H, N–H pyrrole protons 21, 22).

Also in this case, the peak assignments were confirmed by T-ROESY and COSY experiments. In particular, T-ROESY plot (Supplementary data, Fig. 3) shows the cross-peaks correlation between protons a′–(2, 18, 8, 12) and c′–b′, whereas the COSY plot shows some cross-peak correlations between protons (12, 8, 2, 18)–(13, 7, 3, 17), a′–b′, a–b and c–d.

Comparing the NMR signals of cy-[O–(H_2–PTTEG$_2$)–O–CH_2–]$_4$ (Fig. 6a) with those of the corresponding porphyrin HO(H_2–PTTEG$_2$) OH monomer (Fig. 6b), lower chemical shift values of the protons 3, 7, 13, 17, a, b and c (protons enclosed in the areas A of Scheme 3) can be observed. In particular, signals of pyrrole protons 3, 7 and 13, 17 pass from 8.87 and 8.12 ppm (monomer) to 7.68 and 6.83 ppm

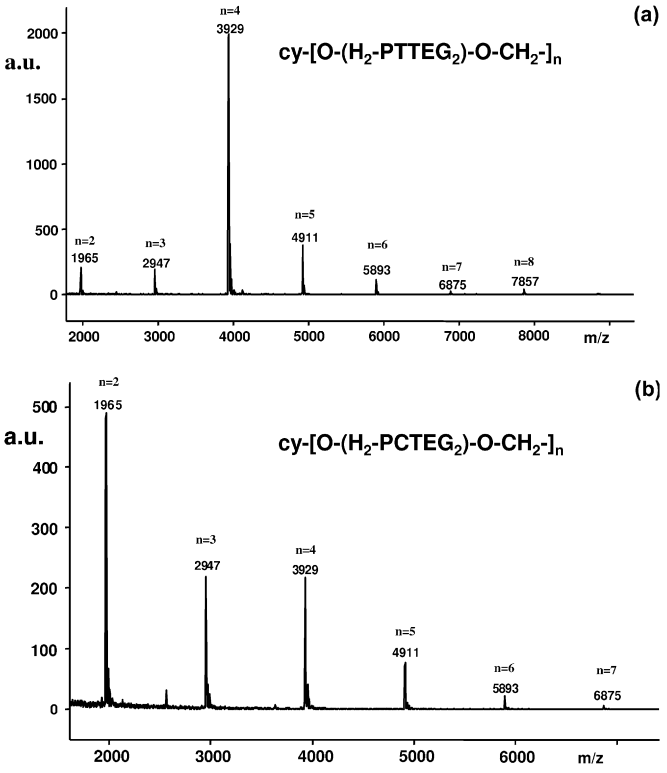

Fig. 2. Positive MALDI-TOF mass spectra of: (a) cy-[O–(H_2–PTTEG$_2$)–O–CH_2–]$_n$; (b) cy-[O–(H_2–PCTEG$_2$)–O–CH_2–]$_n$.

(cyclic tetramer), respectively; analogously, phenyl protons a and b pass from 7.3 ppm to 5.80 ppm and methylene protons c from 4.42 ppm to 3.18 ppm. A minor effect was observed for the aliphatic protons d, e, f, g, h and ω.

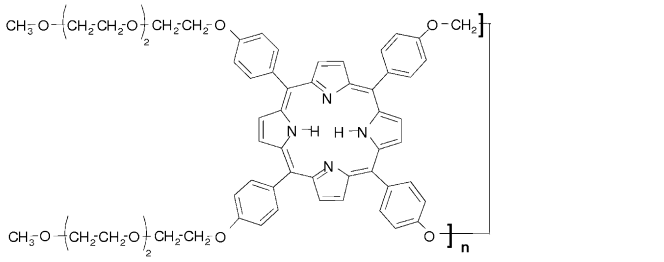

cy-[O-(H_2-PCTEG$_2$)-O-CH_2-]$_n$

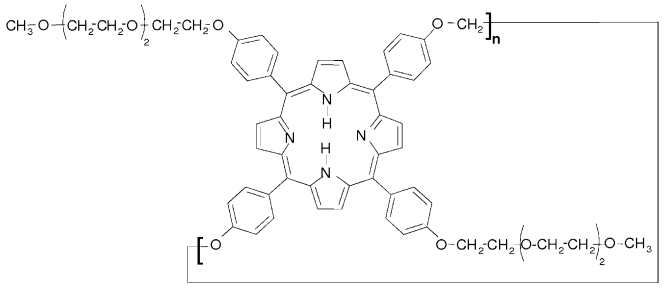

cy-[O-(H_2-PTTEG$_2$)-O-CH_2-]$_n$

Scheme 1. Chemical structure of 10,20-{cy-[O–(H_2–PTTEG$_2$)–O–CH_2–]$_n$} and 15,20-{cy-[O–(H_2–PCTEG$_2$)–O–CH_2–]$_n$} porphyrin oligomers.

On the contrary, a lower field shift phenomenon was observed for the signals of protons a′, b′, 21 and 22 (placed in molecular zone B, see Scheme 3). In fact, protons a′ and b′ appear at 8.29 and 7.68 ppm (cyclic tetramer) instead of 8.08 and 7.23 ppm (monomer) and the protons 21 and 22 at −2.68 ppm rather that −2.77 ppm.

Furthermore, for the open-chain HO[(H_2–PTTEG$_2$)–O–CH_2–]$_m$–(H_2–PTTEG$_2$)OH (spectrum of Fig. 6c) a moderate low field shift of the signals was observed for all the aromatic protons and no shift appeared for all the aliphatic ethyleneoxy protons.

Considering these data, the high-field shift of protons 3, 7, 13, 17, a, b and c (surprisingly not observed for other cyclic oligomers with $n \neq 4$, spectra omitted for brevity) can be supposed due to the structural form of the tetrameric cyclic molecule. As a possible explanation, it can be considered the mutual effect of the interaction of the π orbitals of the four porphyrin units constituting the four faces of a shaped-box molecular structure with the phenylethyleneoxy parts on the upper and lower rims.

The obtained oligomeric cycles were not soluble in water, so to explore their spectroscopic properties, pertinent UV–vis spectra of diluted solutions were recorded in organic solvents. The UV–vis spectrum (omitted for brevity) of cy-[O–(H_2–PCTEG$_2$)–O–CH_2–]$_2$ dimer (Scheme 2) in toluene, consisting of the characteristically intense soret-band (at 422 nm) and four satellite Q-bands (between 500 and 650 nm), is very similar to those of the starting 10,20- and 15,20-di(hydroxyphenyl)porphyrin monomers.

By contrast, the disappearance of the two Q-bands and a discrete red-shift of the signals (with λ_{max} of soret-band at 432 nm and λ_{max} of Q-bands at 561 and 605 nm, respectively) in toluene solution (Fig. 7) are observed for cy-[O–(H_2–PTTEG$_2$)–O–CH_2–]$_2$.

As in previous cases, the red-shift of about 10 nm, observed for the soret-band (λ=432 nm) of the cyclic dimer with respect to the tetramer (λ=422 nm), can be explained considering the electronic interactions of the two porphyrin rings and/or the hybrid orbital deformation (HOD) phenomenon[24] of the two porphyrin π electronic systems forced to a closer co-facial structure.

On the contrary, no red-shift was observed in the UV–vis spectra of 5,15 porphyrin cyclic trimer, tetramer and pentamer oligomers.

The particular molecular structure of cy-[O–(H_2–PTTEG$_2$)–O–CH_2–]$_2$ suggests its use as a nanometric molecular clip, since it can modify the distance between the two porphyrin rings (thus changing the molecular structure from ‘closed’ to ‘open’) by a reversible protonation of the pyrrole cores[25] (thus causing electrostatic repulsion).

To verify the acid triggering propriety, UV–vis spectra of cy-[O–(H_2–PTTEG$_2$)–O–CH_2–]$_2$ solution in CH_2Cl_2 with an increasing amount of CF_3COOH were recorded; the cyclic dimer proved strongly pH-sensitive[26] (similar to many previous studied monoporphyrin derivatives) as indicated by the red-shifts of both soret and Q-bands recorded in UV–vis spectra in acid conditions. In particular, the intensity of the soret-band (at 425 nm) decreases with acid increasing (see Fig. 8). Meanwhile an additional band appears at 450 nm, whose intensity increases gradually while the Q-bands disappear, substituted by a new signal with a λ_{max} at about 673 nm (phenomenon evinced also by a rapid colour change of the solution from red to green).

This spectrophotometric titration also highlighted that the protonation of cy-[O–(H_2–PTTEG$_2$)–O–CH_2–]$_2$ occurs at a lower acid/porphyrin ratio (see titration traces at λ=450 nm in Fig. 8) with respect to the planar cy-[O–(H_2–PCTEG$_2$)–O–CH_2–]$_2$, [HO(H_2–PTTEG$_2$)OH] and [HO(H_2–PCTEG$_2$)OH] species. Analogous to the monoporphyrin systems,[26] the total reversibility of spectrophotometric modifications, by adding basic agents, was also ascertained.

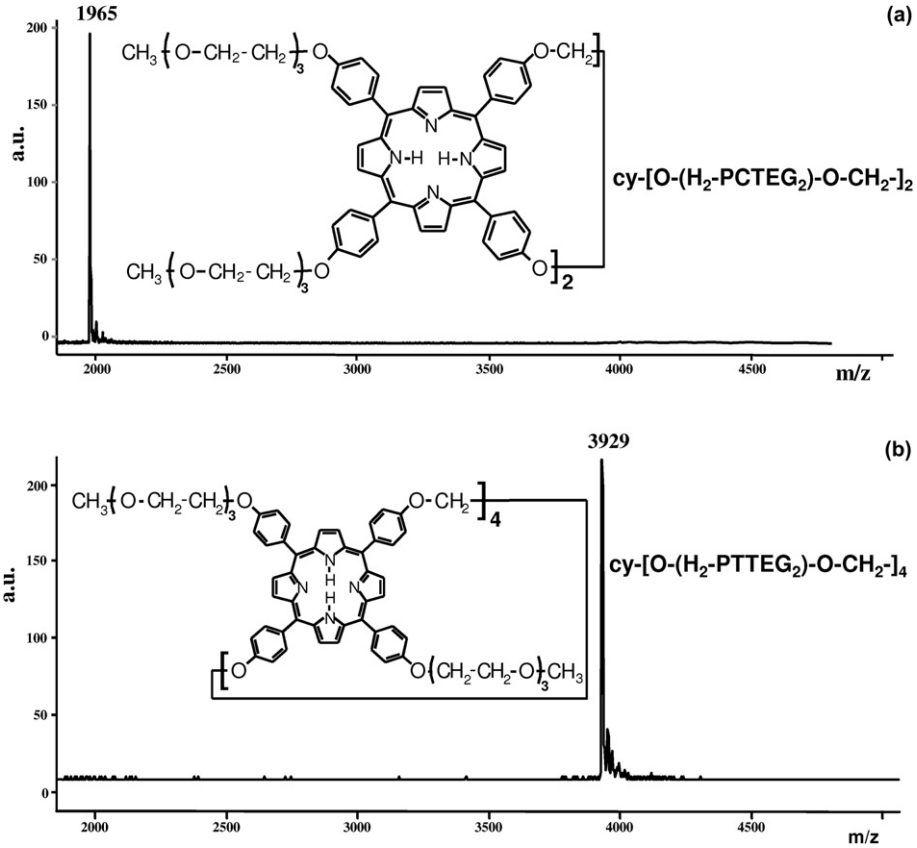

Fig. 3. Positive MALDI-TOF mass spectra of: (a) cy-[O–(H_2–PCTEG_2)–O–CH_2–]$_2$; (b) cy-[O–(H_2–PTTEG_2)–O–CH_2–]$_4$.

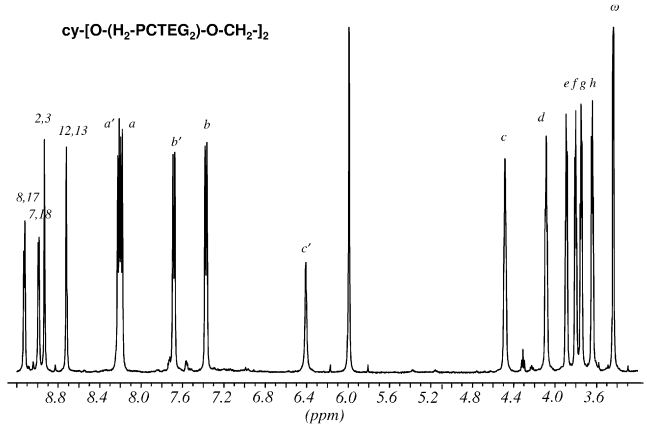

Fig. 4. ^{1}H NMR spectrum ($CDCl_2CDCl_2$, 500 MHz) of cy-[O–(H_2–PCTEG_2)–O–CH_2–]$_2$.

Furthermore, molecular modelling simulation (using molecular mechanics force field calculations) showed that the electrostatic repulsion, induced by means of the protonation of pyrrolic nitrogens, causes a broadening (from about 0.45 nm, Fig. 9a, to about 0.61 nm, Fig. 9b. TEG branches are omitted for clarity.) of the cavity between the co-facial porphyrin rings,[24] so that it could be used as drug-delivery system for tumoral diseases. As a future goal, in acid solution, by diffusion, the drug could be 'loaded' into opened bis-porphyrins and, by a subsequent basic treatment (inducing the closing of the nano-clip), trapped here. After the bis-porphyrin/drug administration, as a result of the strong affinity between porphyrins and tumoral tissues, the complex system can accumulate in neoplastic cells where, finding a lower pH,[27] the drug may be then released for re-opening of the nano-clip.

3. Conclusion

In summary we report the synthesis and NMR, UV–vis and MALDI-TOF characterization of novel cyclic oligomers containing two or four porphyrin units. In particular, in the case of cy-[O–(H_2–PTTEG_2)–O–CH_2–]$_2$ cyclic dimer, the observed UV–vis red-shift of soret and Q-bands was attributed to the hybrid orbital deformation (HOD) phenomenon or to electronic interactions between the two porphyrin rings, forced into a co-facial structure. It was also ascertained that upon acid treatment, the inter-space between the two porphyrins could be reversibly modified by *N*-pyrrole protonation. These data suggest its potential use as a molecular clip for chemical species.

In the case of the cyclic tetramer cy-[O–(H_2–PTTEG_2)–O–CH_2–]$_4$, a ^{1}H NMR high-field shift phenomenon was observed for some signals of aromatic and methyl ether protons, present in the upper and lower of the molecular structure as a consequence of its box-shaped architecture (Fig. 10). The synthesis of corresponding water-soluble compounds and the study of the possible application, as an example, for drug-delivery or as molecular reactors, are in progress.

4. Experimental section

4.1. General

The structures of the cyclic nano-clips and nano-box porphyrin compounds were characterized by ^{1}H NMR analyses. ^{1}H NMR, COSY

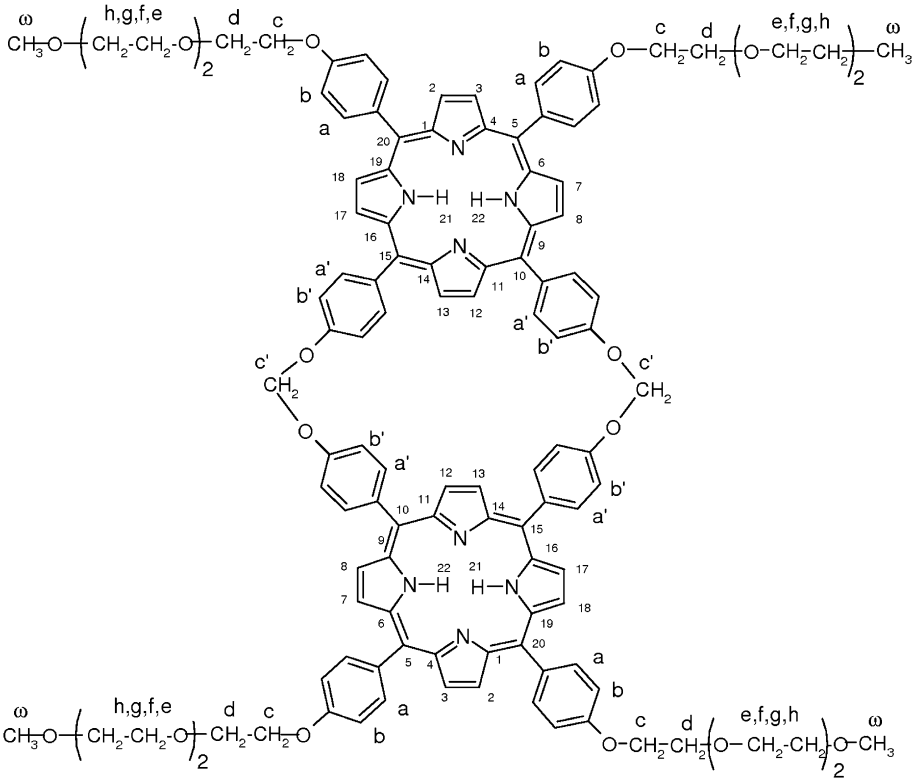

Scheme 2. Chemical structure of cy-[O–(H_2–PCTEG_2)–O–CH_2–]$_2$ porphyrin dimer with proton numeration for ^{1}H NMR assignments.

and T-ROESY spectra were obtained on an ^{UNITY}INOVA Varian instrument operating at 500 MHz (^{1}H) using VNMR for software acquisition and processing. Samples were dissolved in $CDCl_2CDCl_2$ and the chemical shifts were expressed in parts per million compared to the $CHCl_2CHCl_2$ residue signal. The spectra were acquired at 323 K, with a spin lock time of 0.5 s. COSY and T-ROESY spectra were acquired using a Varian standard impulse sequence. In the T-ROESY experiment, a spin lock field of 2000 Hz with a spin lock time of 0.5 s were applied. UV–vis spectra were recorded at room temperature by a Shimadzu Model 1601 spectrophotometer, in quartz cells, using dichloromethane or toluene as a solvent. Positive MALDI-TOF mass spectra were acquired by a Voyager DE-STR (PerSeptive Biosystem) using a simultaneous delay extraction procedure (25 kV applied after 2600 ns with a potential gradient of 454 V/mm and a wire voltage of 25 V) and detection in linear mode. The instrument was equipped with a nitrogen laser (emission at 337 nm for 3 ns) and a flash AD converter (time base 2 ns). *trans*-3-Indoleacrylic acid (IAA) was used as a matrix. Mass spectrometer calibration was performed as reported in previous cases.[28,29] The *m*/*z* values reported in the spectra and in text refer to molecular ions of the most abundant isotope of each element in the molecule. All the solvents and basic materials were commercial products (Sigma–Aldrich) appropriately purified before use.

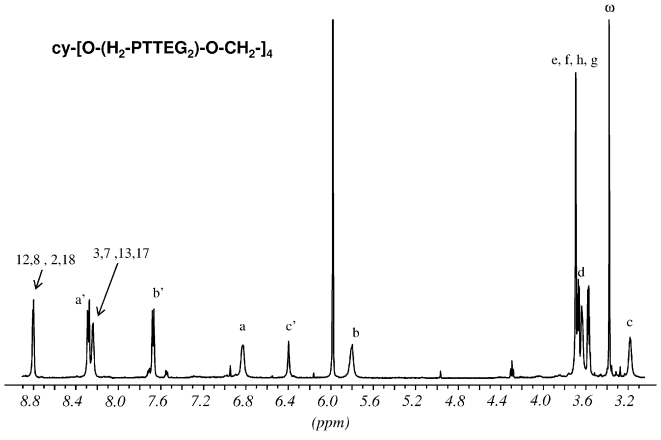

Fig. 5. ^{1}H NMR spectrum ($CDCl_2CDCl_2$, 500 MHz) of cy-[O–(H_2–PTTEG_2)–O–CH_2–]$_4$.

4.2. Synthesis of 5,15-di[*p*-(9-methoxytriethyleneoxy)phenyl]-10,20-di[*p*-hydroxyphenyl]porphyrin [HO(H_2–PTTEG_2)OH] or 5,10-di[*p*-(9-methoxy-triethyleneoxy)phenyl]-15,20-di[*p*-hydroxyphenyl]porphyrin [HO(H_2–PCTEG_2)OH]

Cyclic derivatives were synthesized using 5,15-di[*p*-(9-methoxytriethylenenoxy)phenyl]-10,20-di[*p*-hydroxyphenyl]porphyrin [HO(H_2–PTTEG_2)OH] and 5,10-di[*p*-(9-methoxy-triethylenenoxy)phenyl]-15,20-di[*p*-hydroxyphenyl]porphyrin [HO(H_2–PCTEG_2)OH], two isomeric structures formed in the reaction between tetrakis-*p*-(hydroxyphenyl)porphyrin (obtained from pyrrole and *p*-acetoxybenzaldheyde in boiling propionic acid) and 9-methyltriethyleneoxy chloride (TEGMEC) in aqueous alkaline solution,[19] as reported in the following: in a 100 mL flask, equipped with a reflux condenser, tetrakis-(*p*-hydroxyphenyl)porphyrin (0.3 g, 0.44 mmol) dissolved in 0.5 M NaOH aqueous solution (35 mL) was added under stirring to TEGMEC (0.637 g, 3.5 mmol) dissolved in a H_2O/THF (1/1) mixture (6 mL), and refluxed for 24 h. Then, NaOH and THF (10 mL each) were added and the mixture refluxed for a further 24 h. The products in solution, analyzed by MALDI-TOF mass spectrometry, proved to be a mixture of

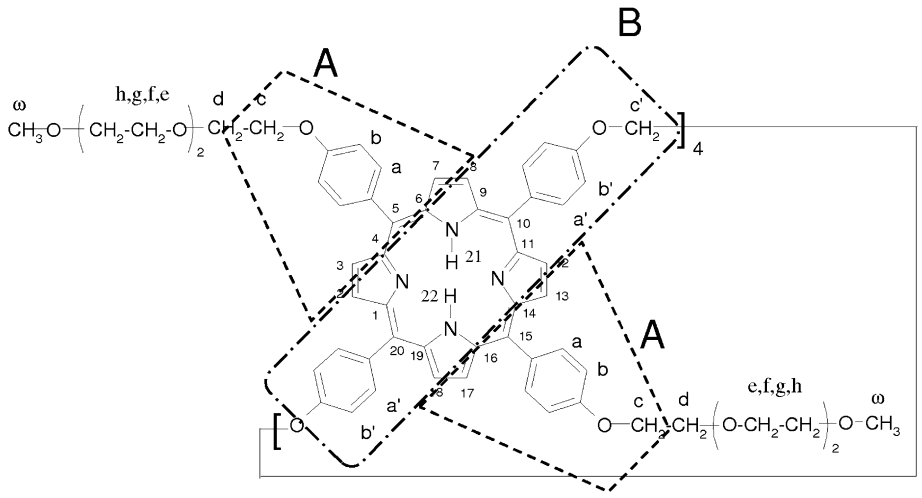

Scheme 3. Chemical structure of cy-[O–(H_2–PTTEG$_2$)–O–CH_2–]$_4$ porphyrin tetramer with proton numeration for ^{1}H NMR assignments.

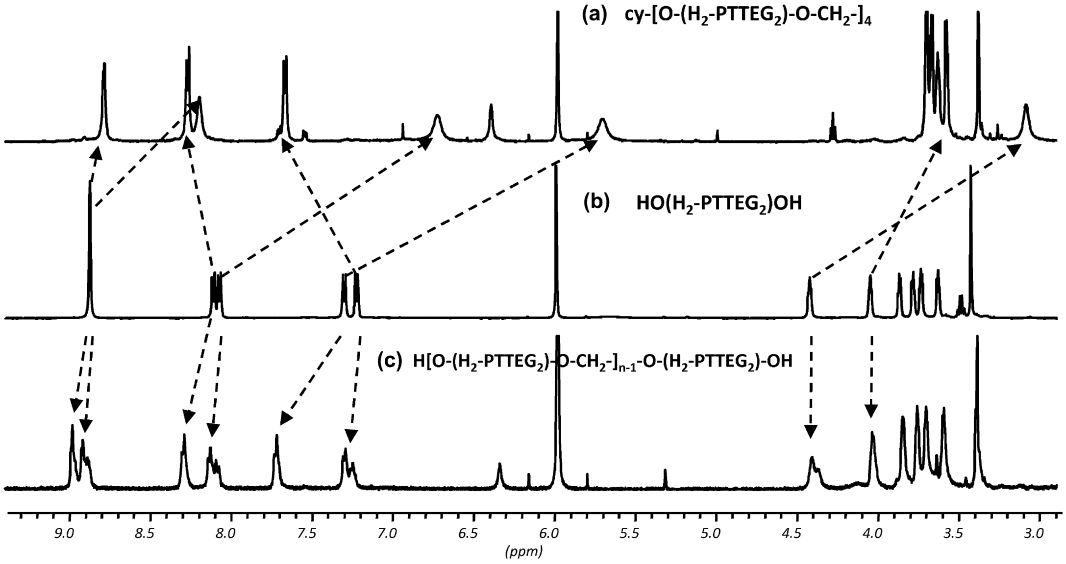

Fig. 6. Comparison of the ^{1}H NMR spectra ($CDCl_2CDCl_2$, 500 MHz) of: (a) cy-[O–(H_2–PTTEG$_2$)–O–CH_2–]$_4$; (b) HO(H_2–PTTEG$_2$)OH; (c) HO[(H_2–PTTEG$_2$)–O–CH_2–]$_m$–(H_2–PTTEG$_2$)OH.

porphyrin derivatives with different numbers of methoxy-triethyleneoxy (TEGME) branches, from which pure products were obtained by chromatographic separation. The solution was slightly acidified with CH_3COOH, dried under vacuum and the residue, dissolved in CH_2Cl_2, fractionated by column chromatography using silica gel as the stationary phase and a mixture of CH_2Cl_2/EtOH/TEA (97/2.5/0.5) as eluant. As indicated by MALDI-TOF analysis (omitted for brevity), the third and fourth coloured compounds eluted from the column (both with MW=970 Da) correspond to two isomeric di-methoxytriethyleneoxy derivatives, obtained with yields of 14% and 26%, respectively, compared to the initial porphyrin amount. ^{1}H NMR, COSY and ROESY analyses (discussed later) helped to identify the third elute as HO(H_2–PTTEG$_2$)OH isomer and the fourth as HO(H_2–PCTEG$_2$)OH isomer.

4.3. Synthesis of ether oligomers

All the reactions were performed under stirring and at refluxing temperature, adopting a suitable reagent molar ratio to promote the formation of low molecular weight oligomeric species and monitoring the reaction progress by TLC and MALDI-TOF mass spectrometry.

4.3.1. Cyclic ether-oligomers. Cy-[O–(H_2–PTTEG$_2$)–O–CH_2–]$_n$ or cy-[O–(H_2–PCTEG$_2$)–O–CH_2–]$_n$, with the porphyrin units linked by methylene bridges (see structures in Scheme 1), were synthesized by interfacial etherification reaction in toluene/H_2O between HO(H_2–PTTEG$_2$)OH or HO(H_2–PCTEG$_2$)OH and a large excess of dibromomethane, with tetrabutyl ammoniumbromide (TBAB) used as phase-transfer agent. In a typical synthetic procedure, TBAB (260 mg, 0.81 mmol) and HO–(H_2–PTTEG$_2$)–OH (100 mg, 0.103 mmol) were dissolved in 2 M NaOH aqueous solution (100 mL) to which CH_2Br_2 (10 mL) dissolved in toluene (80 mL) was added. The mixture was then maintained at reflux under vigorous stirring for 24 h. The material contained in the organic phase was recovered by rotoevaporation in vacuum and the final products were obtained by column chromatography, using silica gel as stationary phase and a CH_2Cl_2/C_2H_5OH (97/3) mixture as eluant (oligomer yield 95%).

4.3.2. Open-chain ether oligomers. By column chromatographic separation of reaction products the fifth fraction collected (a very

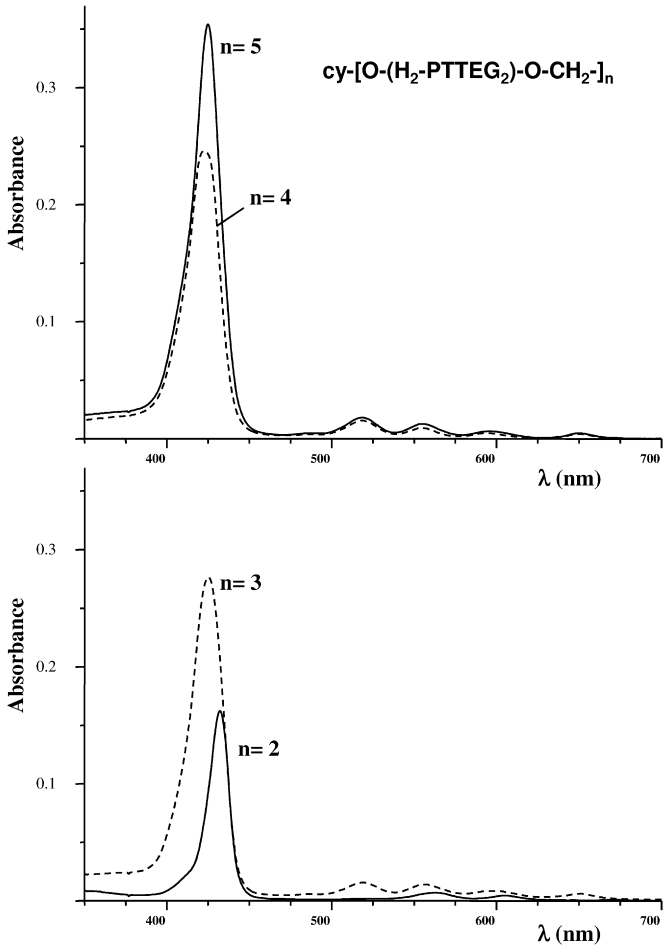

Fig. 7. Comparison among the UV–vis solution spectra in toluene (3.85×10^{-6} M) of cyclic methylene-porphyrin cy-[O–(H_2–PTTEG$_2$)–O–CH_2–]$_n$ ethers with n=2–5.

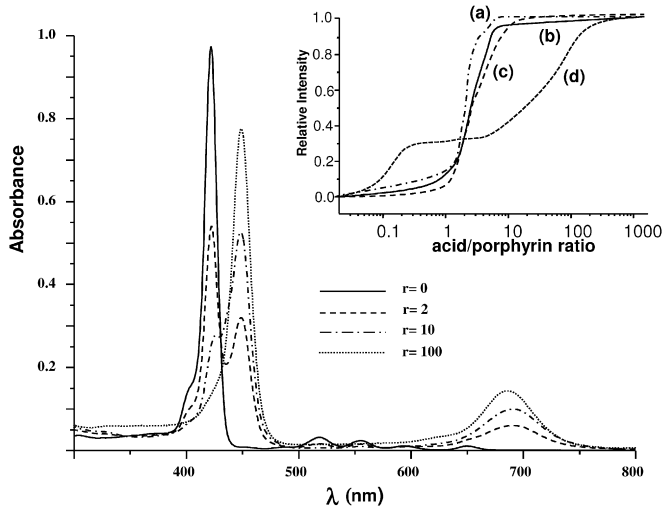

Fig. 8. UV–vis spectra of cy-[O–(H_2–PTTEG$_2$)–O–CH_2–]$_2$ in dichloromethane solution with different amount of CF_3COOH (r=molar ratio between CF_3COOH and porphyrin). In the inset, spectrophotometric titrations at 450 nm of: (a) HO(H_2–PCTEG$_2$)OH; (b) HO(H_2–PTTEG$_2$)OH; (c) cy-[O–(H_2–PCTEG$_2$)–O–CH_2–]$_2$; (d) cy-[O–(H_2–PTTEG$_2$)–O–CH_2–]$_2$ are reported (relative intensity values correspond to UV–vis intensity at 450 nm with respect to full protonated species).

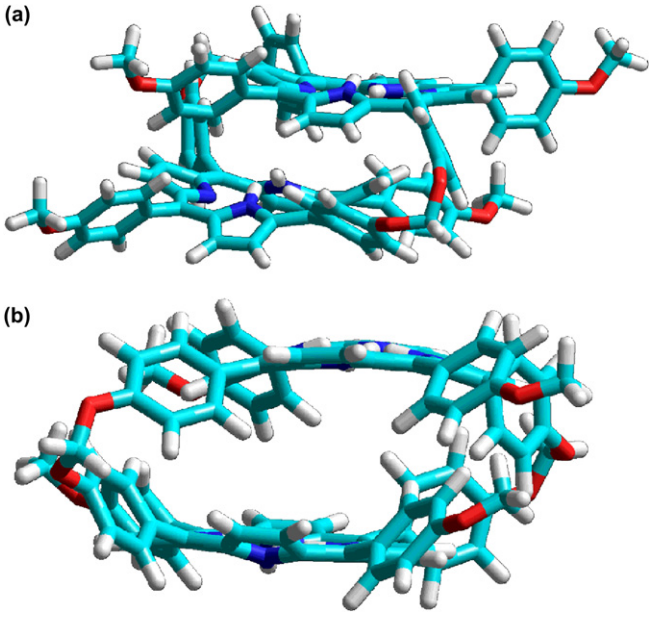

Fig. 9. Molecular model of cyclic dimer cy-[O–(H_2–PTTEG$_2$)–O–CH_2–]$_2$, respectively, as: (a) pure and (b) protonated form.

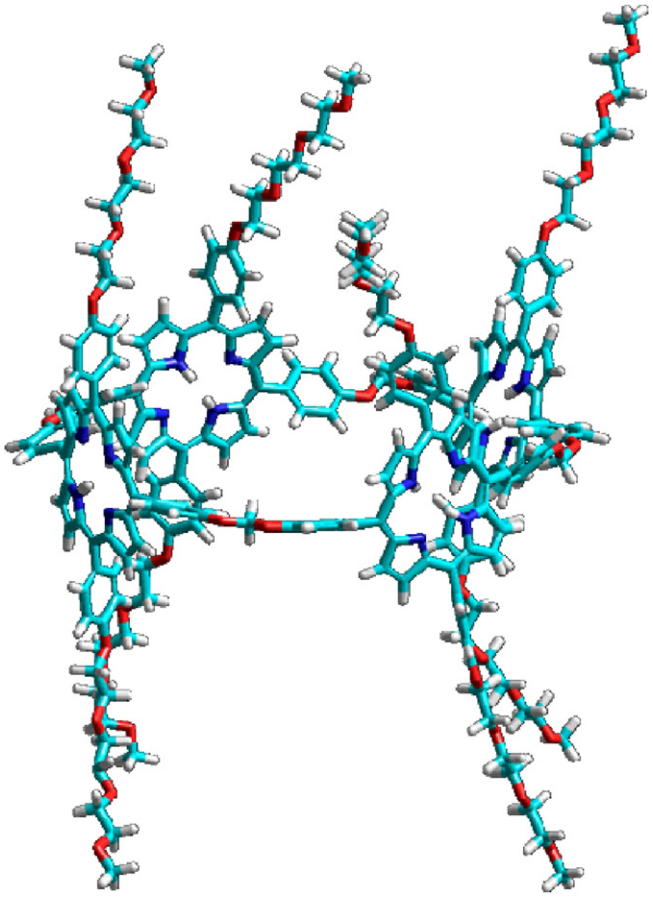

Fig. 10. Molecular model of cyclic tetramer cy-[O–(H_2–PTTEG$_2$)–O–CH_2–]$_4$.

small amount) was a mixture of open-chain HO[(H_2–PTTEG$_2$)–O–CH_2–]$_m$–(H_2–PTTEG$_2$)OH oligomers.

Acknowledgements

The authors thank the Ministero Istruzione Università e Ricerca (MIUR, Roma) for the partial financial support (PRIN 2008—'*New Porphyrins as Chirogenetic Probes to Recognition of Peptides and Proteins of Biological Interest*'—N. Prot. 2008KHW8K4) and the National Research Council (CNR, Roma). Thanks are due to Mr. R. Rapisardi for his contribution to the MALDI-TOF measurements.

Supplementary data

Supplementary data associated with this article can be found in the online version, at doi:10.1016/j.tet.2011.03.072.

References and notes

1. Balaz, M.; De Napoli, M.; Holmes, A. E.; Mammana, A.; Nakanishi, K.; Berova, N.; Purrello, R. *Angew. Chem.* **2005**, *117*, 4074.
2. Pompa, P. P.; Biasco, A.; Cingolani, R.; Rinaldi, R.; Verbeet, M. Ph.; Canters, G. W. *Phys. Rev. E* **2004**, *69*, 032901.
3. Czeslik, C.; Jansen, R.; Ballauff, M.; Wittemann, A.; Royer, C. A.; Gratton, E.; Hazlett, T. *Phys. Rev. E* **2004**, *69*, 021401.
4. D'Urso, A.; Mammana, A.; Balaz, M.; Holmes, A. E.; Berova, N.; Lauceri, R.; Purrello, R. *J. Am. Chem. Soc.* **2009**, *131*, 2046.
5. Awawdeh, M. A.; Legako, J. A.; Harmon, H. J. *Sens. Actuators, B* **2003**, *91*, 227.
6. Aoyama, Y.; Yamagishi, A.; Asagawa, M.; Toi, H.; Ogoshi, H. *J. Am. Chem. Soc.* **1988**, *110*, 4076.
7. Mizutani, T.; Wada, K.; Kitagawa, S. *J. Am. Chem. Soc.* **1999**, *121*, 11425.
8. Mikros, E.; Gaudemer, F.; Gaudemer, A. *Inorg. Chem.* **1991**, *30*, 1806.
9. Verchere-Beaur, C.; Mikros, E.; Perre-Fauvet, M.; Gaudemer, A. *J. Inorg. Biochem.* **1990**, *40*, 127.
10. Borovkov, V. V.; Lintuluoto, J. M.; Inoue, Y. *J. Am. Chem. Soc.* **2001**, *123*, 2979.
11. Kim, Y. H.; Jeong, D. H.; Kim, D.; Jeoung, S. C.; Cho, H. S.; Kim, S. K.; Aratani, N.; Osuka, A. *J. Am. Chem. Soc.* **2001**, *123*, 76.
12. Ambroise, A.; Li, J.; Yu, L.; Lindsey, J. S. *Org. Lett.* **2000**, *2*, 2563; Hwang, I.; Kamada, T.; Ahn, T. K.; Ko, D. M.; Nakamura, T.; Tsuda, A.; Osuka, A.; Kim, D. *J. Am. Chem. Soc.* **2004**, *126*, 16187.
13. Anderson, H. L.; Sanders, J. K. *J. Chem. Soc., Perkin Trans. 1* **1995**, 2223.
14. Anderson, H. L.; Walter, C. J.; Vidal-Ferran, A.; Hay, R. A.; Lowden, P. A.; Sanders, J. K. M. *J. Chem. Soc., Perkin Trans. 1* **1995**, 2275.
15. Hoffmann, M.; Karnbratt, J.; Chang, M.; Herz, L. M.; Albinsson, B.; Anderson, H. L. *Angew. Chem., Int. Ed.* **2008**, *47*, 4993.
16. Kimura, M.; Shiba, T.; Yamazaki, M.; Hanabusa, K.; Shirai, H.; Kobayashi, N. *J. Am. Chem. Soc.* **2001**, *123*, 5636.
17. Bar, A. K.; Chakrabarty, R.; Mostafa, G.; Mukherjee, P. S. *Angew. Chem., Int. Ed.* **2008**, *47*, 8455.
18. Nobukuni, H.; Shimazaki, Y.; Tani, F.; Naruta, Y. *Angew. Chem., Int. Ed.* **2007**, *119*, 9133.
19. Mineo, P.; Vitalini, D.; Scamporrino, E. *Macromol. Rapid Commun.* **2002**, *23*, 681.
20. Mineo, P.; Dattilo, S.; Vitalini, D.; Spina, E.; Scamporrino, E. *Macromol. Rapid Commun.* **2007**, *28*, 1546.
21. Angelini, N.; Micali, N.; Villari, V.; Mineo, P.; Scamporrino, E.; Vitalini, D. *Phys. Rev. E* **2005**, *71*, 21915/1.
22. Angelini, N.; Micali, N.; Mineo, P.; Scamporrino, E.; Villari, V.; Vitalini, D. *J. Phys. Chem. B* **2005**, *109*, 18645.
23. Villari, V.; Mineo, P.; Micali, N.; Angelini, N.; Vitalini, D.; Scamporrino, E. *Nanotechnology* **2007**, *18*, 375503/1.
24. Zhou, Z.; Cao, C.; Liu, Q.; Jiang, R. *Org. Lett.* **2010**, *12*, 1780.
25. Balzani, V.; Credi, A.; Raymo, F. M.; Stoddart, J. F. *Angew. Chem., Int. Ed.* **2000**, *39*, 3348.
26. Gulino, A.; Mineo, P.; Bazzano, S.; Vitalini, D.; Fragalà, I. *Chem. Mater.* **2005**, *17*, 4043.
27. Bae, Y.; Fukushima, S.; Harada, A.; Kataoka, K. *Angew. Chem., Int. Ed.* **2003**, *42*, 4640.
28. Mineo, P.; Vitalini, D.; Scamporrino, E.; Bazzano, S.; Alicata, R. *Rapid Commun. Mass Spectrom.* **2005**, *19*, 2773.
29. Montaudo, G.; Vitalini, D.; Mineo, P.; Scamporrino, E. *Rapid Commun. Mass Spectrom.* **1996**, *10*, 1551; Vitalini, D.; Mineo, P.; Scamporrino, E. *Macromolecules* **1997**, *30*, 5285.